*Journal of Experimental Botany*, Vol. 72, No. 7 pp. 2686–2695, 2021
doi:10.1093/jxb/eraa589 Advance Access Publication 21 December 2020
This paper is available online free of all access charges (see https://academic.oup.com/jxb/pages/openaccess for further details)

RESEARCH PAPER

# Leaf apoplastic alkalization promotes transcription of the ABA-synthesizing enzyme Vp14 and stomatal closure in *Zea mays*

**Christoph-Martin Geilfus[1,*], Xudong Zhang[2,*], Axel Mithöfer[3], Lisa Burgel[2,†], Gyöngyi Bárdos[2] and Christian Zörb[2]**

[1] Division of Controlled Environment Horticulture, Albrecht Daniel Thaer-Institute of Agricultural and Horticultural Sciences, Humboldt-University of Berlin, Albrecht-Thaer-Weg 1, D-14195 Berlin, Germany
[2] Institute of Crop Science, Quality of Plant Products, University Hohenheim, Schloss, Westhof-West, 118, D-70593 Stuttgart, Germany
[3] Max Planck Institute for Chemical Ecology, Research Group Plant Defense Physiology, Hans-Knöll-Straße 8, D-07745 Jena, Germany
[†] Present address: Department of Agronomy, Institute of Crop Science, University Hohenheim, D-70593 Stuttgart, Germany.

* Correspondence: geilfusc@hu-berlin.de or xudong.zhang@uni-hohenheim.de

Received 30 September 2020; Editorial decision 10 December 2020; Accepted 15 December 2020

Editor: Ian Dodd, Lancaster University, UK

## Abstract

**The chloride component of NaCl salinity causes the leaf apoplast to transiently alkalinize. This transition in pH reduces stomatal aperture. However, whether this apoplastic pH ($pH_{apo}$) transient initiates stomatal closure by interacting with other chloride stress-induced responses or whether the pH transient alone initiates stomatal closure is unknown. To clarify the problem, the transient alkalinization of the leaf apoplast was mimicked in intact maize (*Zea mays* L.) by infiltrating near-neutral pH buffers into the leaf apoplast. Effects of the $pH_{apo}$ transient could thus be investigated independently from other chloride stress-derived effects. Microscopy-based ratiometric live $pH_{apo}$ imaging was used to monitor $pH_{apo}$ *in planta*. LC-MS/MS and real-time quantitative reverse transcription–PCR leaf analyses showed that the artificially induced $pH_{apo}$ transient led to an increase in the concentrations of the stomata-regulating plant hormone abscisic acid (ABA) and in transcripts of the key ABA-synthesizing gene *ZmVp14* in the leaf. Since stomatal aperture and stomatal conductance decreased according to $pH_{apo}$, we conclude that the $pH_{apo}$ transient alone initiates stomatal closure. Therefore, the functionality does not depend on interactions with other compounds induced by chloride stress. Overall, our data indicate that the pH of the leaf apoplast links chloride salinity with the control of stomatal aperture via effects exerted on the transcription of ABA.**

**Keywords:** ABA, alkalinization, apoplast, chloride, guard cell, NCED, salinity, stomata, transpiration.

## Introduction

During soil water scarcity, the pH of the leaf apoplast ($pH_{apo}$) is relevant for the regulation of the guard cell pore size. This is because leaf $pH_{apo}$ is implicated in the root to shoot communication of progressive soil drying (Sobeih *et al.*, 2004; Wilkinson and Davies, 2008). A drought stress-induced increase in $pH_{apo}$ links root zone drying with the regulation of

Abbreviations: ABA, abscisic acid; E, transpiration rate; $g_s$, stomatal conductance; NCED, 9-*cis*-epoxycarotenoid dioxygenase; OG, Oregon Green; $pH_{apo}$, apoplastic pH; PM, plasma membrane; qRT–PCR quantitative reverse transcription–PCR; VPD, atmospheric water vapour pressure deficit.

the stomatal aperture by acting on the compartmental distribution of the guard cell-regulating phytohormone abscisic acid (ABA) between the leaf apoplast and symplast (Davies *et al.*, 2002, 2005; Wilkinson and Davies, 2008).

There is, however, an ongoing debate over the site of synthesis of the ABA that accumulates in the leaf in response to soil water scarcity. Some studies conclude that the root is the major site of ABA biosynthesis during soil drying, with root-derived ABA acting as a long-distance chemical signal regulating stomatal conductance (Wilkinson, 1999; Wilkinson *et al.*, 2007; Boyle *et al.*, 2016). New knowledge gained from experiments on reciprocal grafts of ABA-deficient mutants and wild-type (WT) tomato (*Solanum lycopersicum*) plants has challenged this view. Reciprocal grafting experiments with ABA-synthesizing WT and ABA-deficient mutants revealed rootstock independence of stomatal regulation, irrespective of the ABA concentration delivered via the xylem from root to shoot (Holbrook *et al.*, 2002; Dodd *et al.*, 2009; Li *et al.*, 2018). These grafting experiments indicate that rootstock ABA synthesis seems to be less important in regulating leaf ABA concentration and stomatal conductance as the soil dries than originally assumed (Holbrook *et al.*, 2002; McAdam *et al.*, 2016*a*). Instead, a production of ABA in phloem companion cells of the vasculature (Kuromori *et al.*, 2014) might feed the apoplast of water-stressed leaves with ABA, as shown for water-stressed *Arabidopsis thaliana*. In addition, *A. thaliana* guard cell-autonomous ABA synthesis could allow the leaf to maintain hydration (Bauer *et al.*, 2013). In maize, the 9-*cis*-epoxycarotenoid dioxygenase (*NCED*) gene family ortholog *viviparous 14* (*Vp14*) encodes the rate-limiting enzyme in ABA biosynthesis (Seo and Koshiba, 2002; Xiong and Zhu, 2003). The *ZmVp14* gene was characterized from the ABA-deficient maize mutant *Vp14* (Tan *et al.*, 1997) and is known to be regulated by salinity and osmotic stress Geilfus *et al.*, 2018).

For the fraction of the ABA that is not synthesized directly within the guard cell, but has to overcome the leaf apoplastic passage towards the guard cells, the alkalinization of the leaf apoplast or xylem is believed to be important. Such drought stress-induced increases in leaf $pH_{apo}$ and shoot xylem sap pH, respectively, have been shown for field bean (*Vicia faba* L.; Karuppanapandian *et al.*, 2017), maize (*Zea mays* L.; Bahrun *et al.*, 2002), sunflower (*Helianthus annuus* L.; Gollan *et al.*, 1992; Schurr *et al.*, 1992) Asiatic dayflower (*Commelina communis* L.; Wilkinson and Davies, 1997), grapevine (*Vitis vinifera* L.; Stoll *et al.*, 2000), tomato (*Solanum lycopersicum* L.; Wilkinson *et al.*, 1998), hops (*Humulus lupulus* L.; Korovetska *et al.*, 2014), and many others.

However, this drought-induced alkalinization is not universal in all plant species, which has cast doubt on the assumption that it is a ubiquitous long-distance signal that regulates stomatal responses to soil drying (Sharp and Davies, 2009). Of 22 woody perennial species from different plant families, only four (*Buddleja davidii*, *Dicksonia antarctica*, *Penstemon heterophyllus*, and *Rhododendron obtusum*) evolutionarily unrelated species alkalized their xylem sap as the soil dried, but these species showed the greatest control of water status during water scarcity (Sharp and Davies, 2009). Moreover, within eight herbaceous species from various taxonomic groups the ability to alkalinize xylem sap in response to soil drying was not universal, and unrelated to phylogeny (Gloser *et al.*, 2016). Overall, alkalinization was more likely in annual plant species than in woody perennial plants, but there are few insights as to why this is so.

Nevertheless, for those species that alkalinize the apoplast in response to soil drying, the following mode of action is proposed for regulating stomatal aperture. Under well-watered conditions, ABA is released into the leaf apoplast. The apoplastically located ABA is present in its undissociated form (ABAH) because it is a weak acid and because the apoplast is slightly acidic (Hartung, 2010). By following its chemical gradient, the uncharged ABAH diffuses from the leaf apoplast through the plasma membrane (PM) into mesophyll cells. As soon as ABAH enters the slightly alkaline cytosol of the mesophyll, the weak acid dissociates to $ABA^-$ by releasing a proton ($H^+$). The phytohormone is now charged ($ABA^-$) and is trapped inside the mesophyll cells because charged compounds cannot diffuse across the PM (Hartung *et al.*, 1988). It is then stored or metabolized in the mesophyll ( Slovik and Hartung, 1992; Wilkinson and Davies, 1997).

However, during progressive soil drying, the pH of the leaf apoplast increases above the p*K*a of ABA (=4.87) (Karuppanapandian *et al.*, 2017). Thus, under conditions of water scarcity, the ABA that is increasingly delivered from the root or stem dissociates in the leaf apoplast into its charged anionic form, becoming trapped extracellularly (Wilkinson and Davies, 1997). Such a $pH_{apo}$-based accumulation of $ABA^-$ in the leaf apoplast was recently demonstrated under conditions of NaCl salinity when the chloride component of NaCl salinity provoked the leaf apoplast of the field bean to alkalinize over a period of 2–3 h, before it re-acidified once again (Geilfus *et al.*, 2015). After re-acidification of the leaf apoplast back to the initial steady-state pH, the guard cell-intrinsic ABA concentration was increased and the stomata were closed. The guard cell-intrinsic ABA concentration was proposed to rise because the sudden re-acidification of the leaf apoplastic compartment established such a high free proton concentration in the apoplast that the bulk of the apoplastically trapped $ABA^-$ was associated with protons. In other words, a fraction of membrane-permeable ABAH was formed in the leaf apoplast in the vicinity of the guard cells; this ABAH followed its gradient and streamed into the guard cells. This is in good agreement with Goodger *et al.* (2005), who report for maize that the release rates of both ABA and chloride out of mesocotyl xylem sap that is flowing from roots into the shoot correlate with stomatal conductivity. We previously demonstrated that the chloride-induced transient leaf apoplastic alkalinization was instrumental in inducing stomatal closure during the beginning of NaCl salinity through

$pH_{apo}$-based effects on the compartmental distribution of ABA (Geilfus *et al.*, 2015). Experiments with different chloride- or sodium-accompanying counter ions, and with agents that mimicked osmotic stress, revealed that the reduction of the stomatal aperture was linked to the chloride component, namely to the chloride-induced transient leaf apoplastic alkalinization (Geilfus *et al.*, 2015). Nevertheless, stomatal aperture was not reduced when leaf concentrations of chloride increased during the experimental suppression of the formation of the $pH_{apo}$ transient. This was established by clamping the $pH_{apo}$ in the acid range by the infiltration of an acid pH buffer. Hence, the chloride-induced transient alkalinization of the leaf apoplast was inhibited, although chloride was taken up excessively into the leaf. These experiments showed that the $pH_{apo}$ transient mechanistically links chloride stress with a reduction in stomatal aperture (Geilfus *et al.*, 2015).

Nevertheless, these experiments have not revealed whether the formation of the transient apoplastic alkalinization alone, (i) independently from other chloride stress-induced responses and (ii) in the absence of excessive uptake of chloride, is functional in initiating a reduction in stomatal aperture. Only an experimental set-up in which this transient leaf apoplastic alkalinization is mimicked but without stressing the plants with chloride is capable of clarifying this point. With this aim, the chloride-inducible alkalinization of the leaf apoplast was mimicked by infiltrating near-neutral pH buffers in this study. We hypothesized that the formation of this artificially induced $pH_{apo}$ transient reduces stomatal aperture, despite the plants not being salinity stressed, and that ABA synthesis is under control of the $pH_{apo}$ transient. To elaborate these hypotheses, the apoplastic pH dynamics, the transcript abundance of the ABA-synthesizing key enzyme ZmVp14, the abundance of ABA, the stomatal pore size, stomatal conductance ($g_s$), and the transpiration rate (E) were quantified in the leaves of hydroponically gown maize.

## Materials and methods

### Experimental design

Maize (*Zea mays* L.) was cultivated hydroponically in nutrient solution (in 2019 and 2020). To mimic the formation of the transient alkalinization of the leaf apoplast in a way comparable (regarding duration and magnitude) with the chloride-induced alkalinization of the leaf apoplast (see Geilfus *et al.*, 2015), the pH buffer MES (5 mM, pH 6.5) was infiltrated into the leaf apoplast. Ratiometric real-time $pH_{apo}$ imaging was applied to monitor the $pH_{apo}$ transient *in planta* (see below). The pH buffer was mixed with the pH indicator dye Oregon Green (OG) 488-dextran (25 μM) before infiltration. A volume of 0.4 ml of the pH buffer/dye mixture was infiltrated using a needleless syringe. A second experimental group was set up to rule out unspecific effects that may have arisen from the buffering agent (i.e. effects that did not arise from the $pH_{apo}$). For this purpose, 0.4 ml of a mixture of the pH buffer 2-hydroxy-MOPS (MOPSO) (7.5 mM, pH 6.5) and OG dye was infiltrated into the leaf. To guard against effects possibly arising from the infiltration procedure or the infiltration of water, control plants were infiltrated with 0.4 ml of a mixture of water and the OG dye. Osmotic controls were used to test for osmotic effects possibly arising from the pH buffer agents. For this, 0.4 ml of a mixture of the pH buffer MES (7.5 mM, pH 4.7) and OG dye was infiltrated into the leaf. In this fourth experimental group, the pH was set to 4.7 because this proton concentration prevails in the leaf apoplast.

In total, four experimental groups were tested. (i) Control: infiltration of 0.4 ml of an aqueous 25 μM OG solution. (ii) Osmotic control: infiltration of 0.4 ml of a mixture of 7.5 mM MES (pH 4.7) and 25 μM OG. (iii) MES buffer: infiltration of 0.4 ml of a mixture of 5 mM MES (pH 6.5) and 25 μM OG. (iv) MOPSO buffer: infiltration of 0.4 ml of a mixture of 7.5 mM MOPSO (pH 6.5) and 25 μM OG.

To investigate effects of the formation of the artificially induced $pH_{apo}$ transient on the transcription of the ABA-synthesizing maize gene *9-cis-epoxycarotenoid dioxygenase 1* (*ZmVp14*; Tan *et al.*, 2003) and on the abundance of ABA, leaves were sampled at eight key time points to reflect the situation before, during, and after the alkalinization. Microscopy-based live $pH_{apo}$ imaging allowed the identification of these eight time points. A separate batch of plants was necessary for sampling leaf material at each time point. Sampled leaf material was immediately frozen in liquid nitrogen. Since $pH_{apo}$ imaging was performed *in planta* by using a size-calibrated microscope, the size of the stomatal aperture could be quantified concurrently. Transpiration was measured in parallel on separate batches of plants that were treated identically. To confirm that one-time infiltration of 0.4 ml MES or the MOPSO buffers does not disturb the leaf in the long term, we checked rates of photosynthesis and transpiration at 24, 48, and 72 h after infiltration (Supplementary Table S1). For all measurements, the number of biological replicates varied between four and six, as indicated in the figure legends or table captions. Biological replicates represented individual plants taken from different cultivations.

### Plant cultivation

*Zea mays* (cv. Susann, Nordsaat Saatzucht GmbH, Langenstein, Germany) was cultivated in a hydroponic system using a controlled-environment chamber. Seeds were soaked for 1 d before being placed in moistened quartz sand for germination. Four days later, seedlings were transferred into 5 litre plastic pots containing one-quarter strength nutrient solution. After 2 d, the nutrient concentration was increased to half-strength and, after 4 d, to full-strength. The solution was changed every 3.5 d to avoid nutrient depletion. The nutrient solution had the following composition: 1.0 mM $K_2SO_4$, 2.5 mM $Ca(NO_3)_2$, 0.6 mM $MgSO_4$, 0.2 mM $KH_2PO_4$, 1.0 mM $CaCl_2$, 0.01 mM NaCl, 1.0 μM $H_3BO_4$, 2.0 μM $MnSO_4$, 0.3 μM $CuSO_4$, 0.5 μM $ZnSO_4$, 200 μM Fe-EDTA, 0.005 μM $(NH_4)6Mo_7O_{24}$. Plants were cultivated under a 14 h (20 °C):10 h (18 °C) light:dark cycle (photoperiod 08.00–22.00 h) with an atmospheric water vapour pressure deficit (VPD) of 0.58 kPa (75% relative humidity) during the photoperiod. Light intensity was 500 μmol $s^{-1}$ $m^{-2}$ above the leaf canopy. Plants grew for 10 d in full-strength nutrient solution before the $pH_{apo}$ transient was induced by infiltration of the pH buffer.

### Quantification of leaf apoplastic pH and determination of stomatal aperture

Leaf $pH_{apo}$ and stomatal aperture were quantified using a calibrated Leica microscope (Leica DMi8; Leica Microsystems, Wetzlar, Germany). The entire plant was located in a cage incubator system, which allowed the precise control of the VDP (0.58 kPa; 75% relative humidity at 20 °C), and white light illumination via an LED over the entire experiment [light intensity was 400 μmol $m^{-}$ $s^{-1}$ of photosynthetic photon flux density (PPFD)]. LED illumination was automatically switched off during fluorescence image acquisition for $pH_{apo}$ quantification. For the *in vivo* quantification of leaf $pH_{apo}$, a 25 μM solution of the fluorescent pH indicator dye OG 488-dextran (Thermo Fisher Scientific, Darmstadt, Germany) was infiltrated

into the leaf apoplast of intact plants by using a needleless syringe (Geilfus and Mühling, 2011), together with a pH buffer. where applicable. OG 488-dextran is a sensor for $pH_{apo}$ because it does not enter the symplast, as shown by confocal imaging. Fluorescence images for calculation of $pH_{apo}$ were collected as a time series with the Leica DMi8 microscope connected to a cooled sCMOS camera (Leica DFC9000 GT; Leica Microsystems). An HXP lamp (HXP Short Arc Lamp; Osram) was used for illumination at the excitation wavelengths of 440/10 nm and 490/10 nm. The exposure time was 25 ms for both channels. Emission was collected at 535/25 nm by using a band-pass filter in combination with a dichromatic mirror. The fluorescence ratio $F_{490}/F_{440}$ was obtained as a measure of $pH_{apo}$ on a pixel-by-pixel basis. For conversion of the fluorescence ratio data into $pH_{apo}$ values, an *in vivo* calibration was conducted as described elsewhere (Geilfus and Mühling, 2013). Stomatal aperture was quantified off-line on captured images by using the calibrated microscope.

### *RNA extraction, cDNA synthesis, and real-time quantitative RT–PCR*

Forward (f 5'–3': TTCTCGGAGGAGGAACAGAGGA) and reverse (r 5'–3′: CCAACTGTAACTCTGGTGTGCG) primers for amplifying *ZmVp14* mRNA were taken from Geilfus *et al.* (2018). For cDNA synthesis, RNA was isolated from 100 mg of ground lyophilized leaf material by using phenol–chloroform extraction according to the method of Cox and Goldberg (1988). The quality of RNA was checked by $OD_{260}$ and $OD_{280}$. A 1 µg aliquot of total RNA was digested with PerfeCTa DNAseI (Quanta Biosciences, Beverly, MA, USA) to eliminate residual genomic DNA, and reverse transcribed to single-stranded cDNA with the SuperScript VILO cDNA Synthesis Kit (Invitrogen by Life Technologies, Karlsruhe, Germany) according to the manufacturer's instructions. The SYBR-Green-based real-time quantitative reverse transcription–PCR (real-time qRT–PCR) technique was performed on a BioRad CFX96 real-time PCR system by using iTaq Universal SYBR Green Supermix (BioRad Laboratories, Inc.). For each reaction, 0.8 µl of diluted single-stranded cDNA was used in a total volume of 10 µl (0.5 µM forward and reverse primer, 5 µl of iTaq Universal SYBR Green Supermix, topped up with sterilized autoclaved $H_2O_{bidest}$). Cycle information with regard to temperature, time, and cycle number is given in Geilfus *et al.* (2018). The specificity of the annealing was checked by dissociation kinetics performed at the end of the experiment (65–95 °C). The comparative ΔΔCt (threshold cycles) method for relative quantification was used to analyse the data according to Pfaffl (2001). $C_t$ values were normalized by comparison with the two endogenous reference genes actin 1 and ubiquitin-conjugating enzyme. Data are shown as the relative fold changes in transcript expression. Negative controls were carried out without templates. The specificity of the primer–template interactions was demonstrated by sequencing the real-time qRT–PCR products (GATC Biotech, Konstanz, Germany) (Supplementary Table S2). Moreover, agarose gels were run after real-time qRT–PCR to ensure that only a single PCR product was generated and to confirm the predicted PCR product size on the gel (Supplementary Fig. S1).

### *ABA quantification*

Extraction of ABA from the maize leaf was performed by adding 1 ml of extraction solution {5 ng of [$^2H_6$] (+)-*cis*,*trans* ABA internal standard (Olomouc, Czech Republic) in 7:3 methanol:water} to 10 mg of dried ground material. After being shaken for 30 min, samples were centrifuged at 16 000 *g* at 4 °C for 5 min. The supernatant was collected and dried under reduced pressure, re-dissolved in methanol (10 µl per 1 mg DW), mixed, and centrifuged at 16 000 *g* and 4 °C for 10 min. The supernatant was used for the LC-MS/MS-based analysis of ABA (Almeida Trapp *et al.*, 2014).

### *Gas exchange measurements*

A portable gas exchange system (LI-COR 6400 XT; LI-COR) was used to measure $g_s$ (mmol $H_2O$ $m^{-2}$ $s^{-}$) and to obtain rates for E (mmol $H_2O$ $m^{-2}$ $s^{-1}$) and photosynthesis (µmol $CO_2$ $m^{-2}$ $s^{-1}$). PPFD was 500 µmol $m^{-2}$ $s^{-1}$ as provided by the red, green, and blue LEDs of the integrated fluorescence chamber head (6400-02B LED light source; LI-COR). The leaf area included in the chamber was recorded for each leaf. VPD was 0.58 kPa (75% relative humidity; 20 °C). $CO_2$ at a flow rate of 300 µmol $mol^{-1}$ $CO_2$ was controlled by a $CO_2$ injection system.

## Results

### *Infiltrating pH buffers set to pH 6.5 mimics a transient alkalinization of the leaf apoplast*

Infiltrating 0.4 ml of a 5 mM MES solution that was set to a pH of 6.5 into the leaf apoplast immediately increased the leaf $pH_{apo}$ from 4.7 to 6.5 (Fig. 1, green circles). After remaining at pH 6.5 for a period of 80 min, the $pH_{apo}$ started to re-acidify back to the initial steady-state pH of 4.7 over a period of 60 min. A similar transient alkalinization of the leaf apoplast was seen when 0.4 ml of a 7.5 mM MOPSO solution set to a pH of 6.5 was infiltrated into the leaf apoplast (blue diamonds). Control plants that were infiltrated with 0.4 ml of water showed a stable $pH_{apo}$ of 4.7 over the entire experiment (black triangles). The $pH_{apo}$ was also stable at 4.7 when 0.4 ml of a 7.5 mM MES solution set to a pH of 4.7 was infiltrated into the leaf (grey squares). The latter experimental group

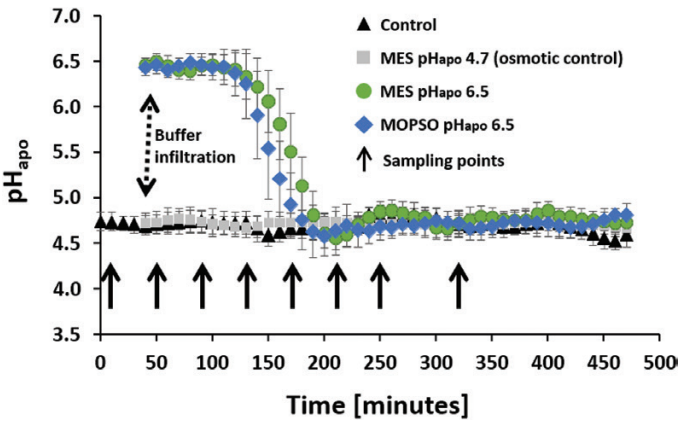


**Fig. 1.** Infiltration of near-neutral pH buffers into the leaf apoplast results in a transient apoplastic alkalinization. Apoplastic pH as plotted over time. Green circles, infiltration of 0.4 ml of a mixture of 5 mM MES at pH 6.5 and 25 µM OG; blue diamonds, infiltration of 0.4 ml of a mixture of 7.5 mM MOPSO at pH 6.5 and 25 µM OG; black triangles, infiltration of 0.4 ml of an aqueous 25 µM OG solution (controls); grey squares, infiltration of 0.4 ml of a mixture of 7.5 mM MES at pH 4.7 and 25 µM OG (osmotic controls). Dashed black arrow, time point of infiltration; solid arrows, time points of the sampling of leaf material for subsequent *vp14* mRNA and ABA quantification. Representative pH kinetics of six equivalent recordings of leaves determined from independent experiments ($n$=6 biological replicates). Quantitation was technically averaged with $n$=4 regions of interest per ratio image and time point (shown as ±SD).

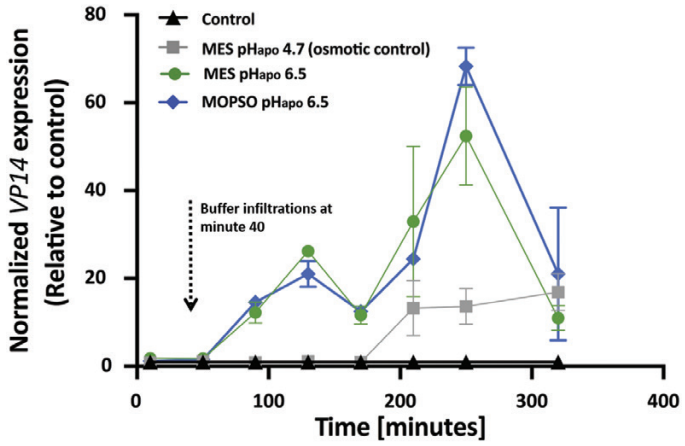


**Fig. 2.** Transient alkalinization of the leaf apoplast increases mRNA abundance of *viviparous 14* (*Vp14*). Increases in transcript abundance shown as fold changes, relative to the control group (being set to 1). Green circles, infiltration of 0.4 ml of a mixture of 5 mM MES at pH 6.5 and 25 µM OG; blue diamonds, infiltration of 0.4 ml of a mixture of 7.5 mM MOPSO at pH 6.5 and 25 µM OG; black triangles, infiltration of 0.4 ml of an aqueous 25 µM OG solution (controls); grey squares, infiltration of 0.4 ml of a mixture of 7.5 mM MES at pH 4.7 and 25 µM OG (osmotic controls). Mean ±SE of four independent (*n*=4) biological replications (technically replicated in triplicate).

served as a control to exclude osmotic effects possibly arising from the infiltration of buffering agents (Fig. 1).

### *Transient alkalinization of leaf apoplast increases abundance of* Vp14 *mRNA*

Infiltration of either MES or MOPSO buffer solutions each set to a pH of 6.5 into the leaf apoplast resulted in a steady increase of the abundance of *Vp14* mRNA, relative to control leaves (Fig. 2). At 210 min after buffer infiltrations (this time point is shown at minute 250 on the *x*-axis), the increases were the highest (52-fold in response to infiltration with MES at pH 6.5 and 68-fold in response to infiltration with MOPSO at pH 6.5). Subsequently, the alkalinization-induced increase in *Vp14* mRNA abundance decreased. Infiltration of the MES buffer set to a pH of 4.7 (osmotic control) resulted in a slight increase of *Vp14* mRNA abundance. In contrast to the alkalinization-induced increase, the osmotically caused increase was detected 120 min later, reaching a much lower maximum that occurred at 280 min after buffer infiltrations (this time point is shown at minute 320 on the *x*-axis) (Fig. 2).

### *Leaf $pH_{apo}$ transient causes leaf ABA concentrations to increase*

Infiltration of either MES or MOPSO buffer solutions each set to a pH of 6.5 into the leaf apoplast resulted in a steady increase of the leaf ABA concentrations, whereas the ABA concentration in the control leaves that were only infiltrated with water remained stable at 20±2 (mean ±SE) ng ABA $g^{-1}$ DW over the entire experiment (Fig. 3A). At 280 min after buffer infiltrations (this time point is shown at minute 320 on the *x*-axis), the increases were at their highest (943±86 ng ABA $g^{-1}$ DW in response to infiltration with MES at pH 6.5 and 1481±59 ng ABA $g^{-1}$ DW in response to infiltration with MOPSO at pH 6.5). Infiltration of MES buffer set to a pH of 4.7 (osmotic control) did not cause a significant increase in ABA concentration (Fig. 3).

### *Transient leaf apoplastic alkalinization reduces stomatal aperture, stomatal conductance, transpiration, and photosynthesis*

At 60 min after infiltration of the pH buffers (this time point is shown at minute 100 on the *x*-axis of Fig. 1) or immediately after the re-acidification (this time point is shown at minute 200 on the *x*-axis of Fig. 1), neither the stomatal aperture (Fig. 3B) nor the stomatal conductance or the transpiration rate (Supplementary Table S3) was influenced by the infiltration of the MES and MOPSO buffer solutions set to a pH of 6.5 (when compared with the control that was infiltrated with water). At 2 h after the apoplast had re-acidified to a pH of 4.7 in response to the infiltration of the MES buffer at pH 6.5 (this time point is shown at minute 320 on the *x*-axis of Fig. 1), however, both the stomatal conductance (128±25 mmol $H_2O$ $m^{-2}$ $s^{-1}$) and the transpiration rate (2.3±0.4 mmol $H_2O$ $m^{-2}$ $s^{-1}$) were significantly lower compared with plants from the control group. In controls, $g_s$ mmol $H_2O$ $m^{-2}$ $s^{-1}$ was 283±45 and E was 5.8±1.1 mmol $H_2O$ $m^{-2}$ $s^{-1}$, (Supplementary Table S3). At the same time point, the stomatal aperture significantly decreased from 108.2±12.8 µm$^2$ to 34.8±8.1 µm$^2$ in response to the MES-induced apoplastic alkalinization (Fig. 3B). Thus, it was significantly lower compared with the control. At 4 h after re-acidification (this time point is shown at minute 440 on the *x*-axis of Fig. 1), the transpiration rate (1.8±0.3 mmol $H_2O$ $m^{-2}$ $s^{-1}$), the stomatal conductance (97±26 mmol $H_2O$ $m^{-2}$ $s^{-1}$), and the stomatal aperture (26.0±5.3 µm$^2$) were still significantly lower in plants from the group 'MES $pH_{apo}$ 6.5' when compared with plants from the control (in the control, E was 6.1±0.9 mmol $H_2O$ $m^{-2}$ $s^{-1}$, $g_s$ was 294±48 mmol $H_2O$ $m^{-2}$ $s^{-1}$, and stomatal aperture was 123.4±14.2 µm$^2$). Similar responses were observed when the leaf apoplast was transiently alkalinized by using the MOPSO buffer set to pH 6.5, when compared with the control. The transpiration rate significantly decreased to 1.7±0.1 mmol $H_2O$ $m^{-2}$ $s^{-1}$ or 1.9±0.3 mmol $H_2O$ $m^{-2}$ $s^{-1}$ at 2 h or 4 h after re-acidification. Stomatal conductance significantly decreased to 85.3±14 mmol $H_2O$ $m^{-2}$ $s^{-1}$ or 102.26±26 mmol $H_2O$ $m^{-2}$ $s^{-1}$ at 2 h or 4 h after re-acidification (Supplementary Table S3). Stomatal aperture significantly decreased to 24.3±6.7 µm$^2$ or 23.1±4.4 µm$^2$ at 2 h or 4 h after re-acidification (Fig. 3B). In good agreement with the stomatal closure that was elicited by the apoplastic alkalinization, the rate of photosynthesis also decreased in response to the alkalinization at the same time points (Supplementary Table

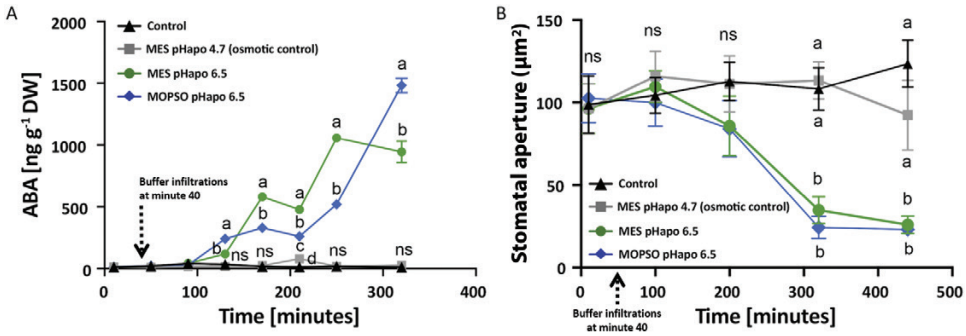


**Fig. 3.** Artificially induced $pH_{apo}$ transient increases leaf ABA concentration and reduces stomatal aperture. (A) Leaf ABA concentration; (B) stomatal aperture. Green circles, infiltration of 0.4 ml of a mixture of 5 mM MES at pH 6.5 and 25 µM OG; blue diamonds, infiltration of 0.4 ml of a mixture of 5 mM MOPSO at pH 6.5 and 25 µM OG; black triangles, infiltration of 0.4 ml of an aqueous 25 µM OG solution (controls); grey squares, infiltration of 0.4 ml of a mixture of 7.5 mM MES at pH 4.7 and 25 µM OG (osmotic controls). For ABA data: mean ±SE of four independent ($n$=4) biological replications (technically replicated in triplicate). Statistical significance ($P$≤0.05) between groups per time point as indicated by Tukey HSD test is shown by letters. For stomatal aperture data: mean ±SD of six independent ($n$=6) biological replications. Statistical significance ($P$≤0.05) between groups per time point as indicated by Tukey HSD test is shown by letters.

S3). Use of osmotic controls revealed that all these effects were not related to the osmotic properties of the buffer solutions: infiltration of a MES buffer set to a pH of 4.5 did not significantly affect stomatal aperture (Fig. 3B) or stomatal conductance and rate of transpiration (Supplementary Table S3).

### *The $pH_{apo}$-induced increase in ABA correlates positively with the decrease in $g_s$*

The Pearson correlation coefficient shows a strong statistical linear relationship between the increasing leaf ABA concentration and the decreasing stomatal conductance only when the apoplast was alkalinized (Pearson $r$= –82 for 'MES $pH_{apo}$ 6.5'; Pearson $r$= –95 for 'MOPSO $pH_{apo}$ 6.5'; data not shown). There was a much weaker (Pearson $r$= –59) or no (Pearson $r$=0.06) statistical relationship between both parameters in plants of the osmotic control or the water control, respectively (data not shown). The $pH_{apo}$ effect on both stomatal conductance and ABA concentration becomes evident when fitting a single relationship between data points from all four experimental groups: Pearson $r$ is –97 (Fig. 4) whereby plants from experimental groups with a re-acidified leaf apoplast ('MES $pH_{apo}$ 6.5', 'MOPSO $pH_{apo}$ 6.5') clearly clustered away from groups where $pH_{apo}$ did not change over the experiment ('control' or 'osmotic control").

## Discussion

Soil salinization is a big constraint for plants because, among other mechanisms, it reduces the availability of water in the soil. Thus, salt and water stress have much in common (Munns, 2002). To maintain turgor and tissue hydration, the plant adjusts its transpiration. With regard to this, the pH of the apoplast is considered to act as a long-distance signal that transmits information about the decreasing soil water availability from root to shoot (Wilkinson, 1999; Wilkinson and Davies, 2008; Geilfus *et al.*, 2015). Upon arrival in the shoot, it regulates stomatal aperture by acting on the compartmental distribution of ABA between the shoot apoplast and symplast (Wilkinson, 1999; Davies *et al.*, 2002). In addition to this Henderson–Hasselbalch-regulated partitioning of ABA (Sharp and Davies, 2009), the present study demonstrates for the first time that the stomatal closure, elicited by the apoplastic alkalinization, is also due to a $pH_{apo}$-mediated increase in the transcription of the NCED gene *Vp14* in the leaf. *ZmVp14* encodes the rate-limiting enzyme in ABA biosynthesis (Seo and Koshiba, 2002).

First of all, the study aimed at clarifying whether this leaf $pH_{apo}$ transient is only functional with regard to the initiation of stomatal closure when interacting in concert with chloride ions or other chloride stress-related responses or variables that are induced by chloride salinity. These could include changes in $[Ca^{2+}]$, $[H_2O_2]$, [ATP], or membrane potential. Following the concept of network signalling (Jordan, *et al.*, 2000; Plieth, 2016), all these variables (signals) would be integrated at downstream junctions to modulate the output (i.e. stomatal closure). Alternatively, the $pH_{apo}$ transient alone might initiate a cascade of events that regulates aperture following the concept of single-file signalling (see Plieth, 2016). The latter proposition suggests that the $pH_{apo}$ transient acts independently from other chloride stress-associated responses that are induced by chloride salinity.

To clarify this, we mimicked the transient alkalinization of the leaf apoplast, as occurs under conditions of chloridestress (of course, without adding chloride stress), by infiltrating near-neutral pH buffers (pH 6.5) into the leaf apoplast. By these means, we investigated the effect of the $pH_{apo}$ transient independently from any chloride stress-derived responses; that is, unrelated to the excessive accumulation of chloride (or its accompanying cation). If the hypothesis that the $pH_{apo}$ transient alone is able to initiate stomatal closure without interacting with other chloride stress-related responses is true, then we

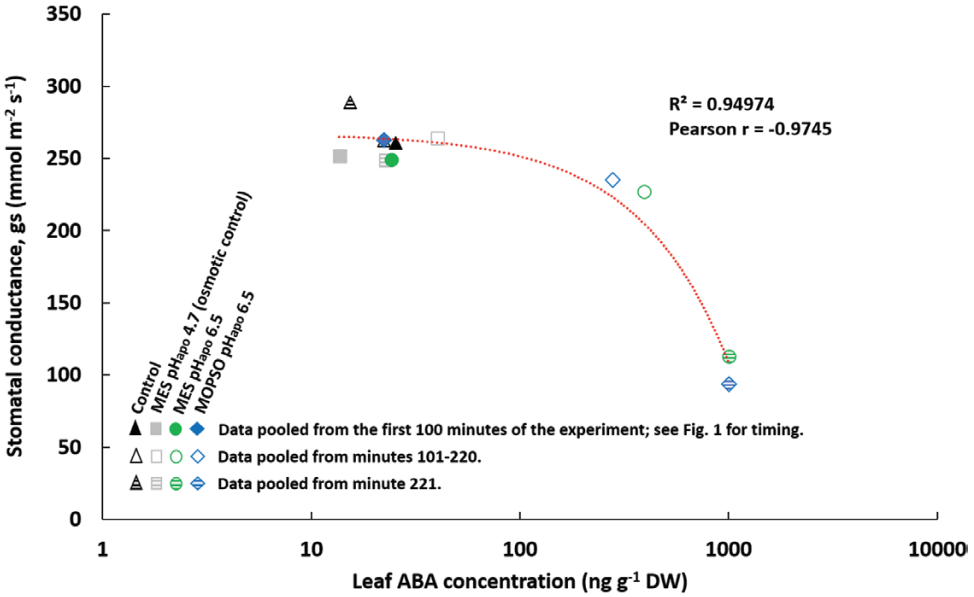


**Fig. 4.** Correlation analysis of stomatal conductance and leaf ABA concentration. Circles, infiltration of 0.4 ml of a mixture of 5 mM MES at pH 6.5 and 25 µM OG; diamonds, infiltration of 0.4 ml of a mixture of 5 mM MOPSO at pH 6.5 and 25 µM OG; triangles, infiltration of 0.4 ml of an aqueous 25 µM OG solution (controls); squares, infiltration of 0.4 ml of a mixture of 7.5 mM MES at pH 4.7 and 25 µM OG (osmotic controls). Filled symbols, data were collected and pooled from the first 100 min of the experiment (please see *x*-axis in Fig. 1 to relate this phase to the leaf apoplastic pH); open symbols, data were collected and pooled from minutes 101 to 220; dashed symbols, data were collected and pooled from minute 221. Results of correlation analysis are indicated by the Pearson correlation coefficient *r*.

would expect that guard cell aperture and stomatal conductance would decrease in response to mimicking the chloride-induced $pH_{apo}$ transient.

### *$pH_{apo}$ transient increases transcript abundance of the* Vp14 *gene in maize leaves*

To stimulate transient leaf apoplastic alkalinization in a similar way to that observed for chloride salinity, a MES-based pH buffer (pH 6.5) was infiltrated into the maize leaf apoplast (Fig. 1). To link this mimicked $pH_{apo}$ dynamic with the synthesis of ABA, the transcript abundance of the ABA-synthesizing gene *ZmVp14* (Tan *et al.*, 2003) was analysed. Relative to the control, the *ZmVp14* transcript abundance increased by up to 52-fold (Fig. 2). To demonstrate that this effect was due to changes in the $pH_{apo}$ and not from the buffering agent MES, a different buffer (MOPSO set to pH 6.5) was infiltrated in a repeat experiment. Relative to the control, *ZmVp14* transcript abundance increased by up to 68-fold (Fig. 2). Infiltration of an osmotic control (i.e. 7.5 mM MES solution that was set to a pH of 4.7) showed that it is the apoplastic pH transient that is responsible for the fast and steep increase in the transcription of the *Vp14* gene in maize, being unrelated to the osmotic properties of the buffer agents (Fig. 2). Any mechanical effects arising from the infiltration procedure or from flooding the apoplast with water can be excluded because controls were infiltrated with water and the above-mentioned fold changes were expressed relative to these controls. It has long been assumed that xylem-transported ABA, which was synthesized in the roots, is of major relevance for the shoot ABA pool when the plants experiences salt stress at the roots. The presented data on *Vp14* gene transcription demonstrated that the leaf is the key site of ABA synthesis, challenging the paradigm that the vast amount of the foliar-located ABA is produced in the roots. Reciprocal grafting experiments with ABA biosynthetic mutant and WT plants suggest that there is a signal that carries the information of a declining root water potential through the xylem to the leaves (Holbrook *et al.*, 2002; Christmann *et al.*, 2007). Upon arrival, leaf hydration, leaf ABA status, and stomatal aperture are adjusted (Manzi *et al.*, 2015; McAdam *et al.*, 2016*a*, *b*, *c*). The leaf apoplastic alkalinization, that travels systemically and acropetally through the shoot (Geilfus *et al.*, 2015), appears to be a candidate for transmitting information about the onset of water scarcity because it induces leaf ABA synthesis (Figs 3, 4) and elicits stomatal closure (Supplementary Table S3).

### *Transient apoplastic alkalinization modulates ABA and increases it in maize leaves*

Next, we investigated whether the artificially induced leaf apoplastic alkalinization was associated with a rise in leaf ABA concentration. A shift in leaf apoplastic pH to 6.5 by means of MES and MOPSO infiltration caused the ABA concentrations steadily to increase steadily over the entire experiment relative to the water control and the osmotic control (Fig. 3). A temporal comparison (compare Fig. 2 and Fig. 3A) reveals that the

increase of the *Vp14* mRNA abundance preceded the increase of the ABA concentration. This indicates that the increase in leaf ABA was caused by increased biosynthesis. However, the means by which the $pH_{apo}$ transient is associated with *Vp14* expression awaits clarification. Is a pH sensor involved? Such a putative sensor would need a pH-responsive (apoplastic-located) domain as part of an integral protein that spans the entirety of the PM. It would sense changes in the $pH_{apo}$ or the transmembrane pH gradient, passing on the information to start signal transduction via intermediate cellular transmitters that finally involve *Vp14* promoter elements. Because the existence of such a sensor is unclear, the elucidation of this problem is extremely difficult. Thus, other explanations have to be taken into consideration. For instance, large changes in the $pH_{apo}$ are known to be able to influence the cytosolic pH (Monshausen *et al.*, 2007). Since cytosolic pH dynamics are accompanied by cellular $Ca^{2+}$ transients (Monshausen *et al.*, 2008, 2009; Michard *et al.*, 2016; Dindas *et al.*, 2018) and have been implicated in the specificity of $Ca^{2+}$ signalling (Behera *et al.*, 2018), large transients in the $pH_{apo}$ might affect ABA transcription via cellular signal transduction. However, such a sequence of events remains speculative unless a clear link between $pH_{apo}$ transients, $Ca^{2+}$ transients, and the induction of *Vp14* gene expression is established. Currently, the transcription of the *NCED* gene is known to be regulated by light (study on tomato by Thompson *et al.*, 2000), salinity and osmotic stress (study on maize by Geilfus *et al.*, 2018), water deficit (study on maize by Tan *et al.*, 1997), and drought (study on *Citrus* by Agustí *et al.*, 2007).

### *Apoplastic alkalinization reduces stomatal aperture and transpiration rate*

Wilkinson and Davies (2008) treated leaves of an ABA-deficient tomato mutant with alkaline-buffered foliar sprays and demonstrated that an increase in the leaf $pH_{apo}$ reduced stomatal conductance only when ABA was simultaneously sprayed onto the leaves of the ABA-deficient tomato. They and others postulated that the apoplastic alkalinization required ABA to act on stomatal aperture (Wilkinson and Davies, 1997, 2008; Sobeih *et al.*, 2004; Else *et al.*, 2006; Jia and Davies, 2007) and suggested a $pH_{apo}$-based mechanism whereby the rise in $pH_{apo}$ increased the amount of ABA that penetrated into the guard cells by changing the compartmental distribution of ABA between the apoplast, the symplast, and various symplastic components.

The presented study adds knowledge about this system as it demonstrates that it is indeed the leaf apoplastic alkalinization that induces *Vp14* gene expression (Fig. 2), presenting a further mechanism that causes the foliar ABA level to rise (Fig. 3A) and stomatal conductance to decline (Fig. 4). This novel finding provides a compelling explanation for the observed stomatal closure and the decline in photosynthetic rate (Supplementary Table S3) elicited by the apoplastic alkalinization.

Apoplastic alkalinization can also be argued to induce stomatal closure directly via $pH_{apo}$-based effects on guard cell $K^+$ fluxes. A rising pH in the stomatal cavity decreases the activity of guard cell-localized inwardly rectified $K^+$ channels and increases the activity of guard cell-localized outwardly rectified $K^+$ channels (Hedrich *et al.*, 1995; Ache *et al.*, 2000). However, two arguments oppose the assumption that stomata close because of the direct $pH_{apo}$-based stimulation of outwardly rectified guard cell $K^+$ channels, highlighting the role of a $pH_{apo}$-based effect of ABA biosynthesis. First, both the stomatal aperture and the transpiration rate remained reduced at 4 h after re-acidification (Supplementary Table S3). During these 4 h, the plants were continuously illuminated with white light. As light increases the activity of inwardly rectified $K^+$ channels (Roelfsema and Hedrich, 2005; Marten *et al.*, 2007), enough time would have been available for a light-induced $K^+$ influx to mediate the re-opening of the stomata. However, the stomatal aperture remained reduced. Second, the stomatal aperture and transpiration remained reduced, although the apoplast had become acidified once again, over the 4 h, to a $pH_{apo}$ range that favoured $K^+$ influx into guard cells via inwardly rectified $K^+$ channels; such changes could ultimately result in guard cell re-opening, if not blocked by ABA.

### *Conclusions*

We have shown that an artificially induced transient of the pH of the leaf apoplast initiates stomatal closure and reduces the rate of leaf transpiration (Supplementary Table S3). A $pH_{apo}$-based *de novo* synthesis of the guard cell-regulating hormone ABA in leaves (Fig. 2) and a $pH_{apo}$-based increase of leaf ABA concentration (Fig. 3) may be the reason for the reduced leaf transpiration rate; that is, the reduction in stomatal conductance (Fig. 4). Our first novel finding is that the pH of the apoplast increases the transcription of *Vp14*, a gene that is key for ABA synthesis in maize. The second novelty is that the functionality of the $pH_{apo}$ transient with respect to reducing the rate of transpiration does not depend on interactions with compounds that are induced by chloride stress. These findings are relevant, since the transient alkalinization of the leaf apoplast is a widespread phenomenon that occurs not only under chloride salinity, but also in response to drought (Bacon *et al.*, 1998) or leaf infections with *Blumeria graminis* (Felle *et al.*, 2008) or *Piriformospora indica* (Felle *et al.*, 2009). Future studies should compare plant species that show the apoplastic alkalization with plant species that do not, in order to understand the underlying mechanism(s) of the transient shift in the apoplastic pH.

## Supplementary data

The following supplementary data are available at *JXB* online.

Table S1. Effect of infiltration on photosynthetic rate.

Table S2. Specificity of the *ZmVp14* primer pair was demonstrated by sequencing the real-time quantitative RT–PCR product.

Table S3. $pH_{apo}$ transient reduces transpiration rate, stomatal conductance, and photosynthetic rate

Fig. S1. Specificity of the *Vp14* primer pair.

## Acknowledgements

This work was supported by a Deutsche Forschungsgemeinschaft research grant (GE 3111/1-1), which is gratefully acknowledged. We thank the editor Prof. Dr. Ian Dodd for extensive advice on the manuscript.

## Author contributions

CMG conceived the project and designed the experiments; CMG, XZ, AM, LB, and GB carried out the experiments; CMG and XZ analysed the data; CMG wrote the manuscript with valuable input from AM, CZ, and XZ. All authors read and approved the final manuscript.

## Data availability

All data supporting the findings of this study are available within the paper and within its supplementary data published online.

## References

**Ache P, Becker D, Ivashikina N, Dietrich P, Roelfsema MR, Hedrich R.** 2000. GORK, a delayed outward rectifier expressed in guard cells of *Arabidopsis thaliana*, is a $K^+$-selective, $K^+$-sensing ion channel. FEBS Letters **486**, 93–98.

**Agustí J, Zapater M, Iglesias DJ, Cercós M, Tadeo FR, Talón M.** 2007. Differential expression of putative 9-cis-epoxycarotenoid dioxygenases and abscisic acid accumulation in water stressed vegetative and reproductive tissues of citrus. Plant Science **172**, 85–94.

**Almeida Trapp M, De Souza GD, Rodrigues-Filho E, Boland W, Mithöfer A.** 2014. Validated method for phytohormone quantification in plants. Frontiers in Plant Science **5**, 417.

**Bacon MA, Wilkinson S, Davies WJ.** 1998. pH-regulated leaf cell expansion in droughted plants is abscisic acid dependent. Plant Physiology **118**, 1507–1515.

**Bahrun A, Jensen CR, Asch F, Mogensen VO.** 2002. Drought-induced changes in xylem pH, ionic composition, and ABA concentration act as early signals in field-grown maize (*Zea mays* L.). Journal of Experimental Botany **53**, 251–263.

**Bauer H, Ache P, Lautner S, *et al.*** 2013. The stomatal response to reduced relative humidity requires guard cell-autonomous ABA synthesis. Current Biology **23**, 53–57.

**Behera S, Zhaolong X, Luoni L, Bonza MC, Doccula FG, De Michelis MI, Morris RJ, Schwarzländer M, Costa A.** 2018. Cellular $Ca^{2+}$ signals generate defined pH signatures in plants. The Plant Cell **30**, 2704–2719.

**Boyle RK, McAinsh M, Dodd IC.** 2016. Stomatal closure of *Pelargonium* × *hortorum* in response to soil water deficit is associated with decreased leaf water potential only under rapid soil drying. Physiologia Plantarum **156**, 84–96.

**Christmann A, Weiler EW, Steudle E, Grill E.** 2007. A hydraulic signal in root-to-shoot signalling of water shortage. The Plant Journal **52**, 167–174.

**Cox K, Goldberg R.** 1988. Isolation of total RNA. In: Shaw CH, ed. Plant molecular biology: a practical approach. Oxford: IRL Press, 2–8.

**Davies WJ, Kudoyarova G, Hartung W.** 2005. Long-distance ABA signaling and its relation to other signaling pathways in the detection of soil drying and the mediation of the plant's response to drought. Journal of Plant Growth Regulation **24**, 285.

**Davies WJ, Wilkinson S, Loveys B.** 2002. Stomatal control by chemical signalling and the exploitation of this mechanism to increase water use efficiency in agriculture. New Phytologist **153**, 449–460.

**Dindas J, Scherzer S, Roelfsema MRG, von Meyer K, Müller HM, Al-Rasheid K, Palme K, Dietrich P, Becker D, Bennett MJ.** 2018. AUX1-mediated root hair auxin influx governs SCF TIR1/AFB-type $Ca^{2+}$ signaling. Nature Communications **9**, 1174.

**Dodd IC, Theobald JC, Richer SK, Davies WJ.** 2009. Partial phenotypic reversion of ABA-deficient flacca tomato (*Solanum lycopersicum*) scions by a wild-type rootstock: normalizing shoot ethylene relations promotes leaf area but does not diminish whole plant transpiration rate. Journal of Experimental Botany **60**, 4029–4039.

**Else MA, Taylor JM, Atkinson CJ.** 2006. Anti-transpirant activity in xylem sap from flooded tomato (*Lycopersicon esculentum* Mill.) plants is not due to pH-mediated redistributions of root- or shoot-sourced ABA. Journal of Experimental Botany **57**, 3349–3357.

**Felle HH, Herrmann A, Schäfer P, Hückelhoven R, Kogel KH.** 2008. Interactive signal transfer between host and pathogen during successful infection of barley leaves by *Blumeria graminis* and *Bipolaris sorokiniana*. Journal of Plant Physiology **165**, 52–59.

**Felle HH, Waller F, Molitor A, Kogel KH.** 2009. The mycorrhiza fungus *Piriformospora indica* induces fast root-surface pH signaling and primes systemic alkalinization of the leaf apoplast upon powdery mildew infection. Molecular Plant-Microbe Interactions **22**, 1179–1185.

**Geilfus CM, Ludwig-Müller J, Bárdos G, Zörb C.** 2018. Early response to salt ions in maize (*Zea mays* L.). Journal of Plant Physiology **220**, 173–180.

**Geilfus CM, Mithöfer A, Ludwig-Müller J, Zörb C, Muehling KH.** 2015. Chloride-inducible transient apoplastic alkalinizations induce stomata closure by controlling abscisic acid distribution between leaf apoplast and guard cells in salt-stressed *Vicia faba*. New Phytologist **208**, 803–816.

**Geilfus CM, Mühling KH.** 2011. Real-time imaging of leaf apoplastic pH dynamics in response to NaCl stress. Frontiers in Plant Science **2**, 13.

**Geilfus CM, Mühling KH.** 2013. Ratiometric monitoring of transient apoplastic alkalinizations in the leaf apoplast of living *Vicia faba* plants: chloride primes and PM-$H^+$-ATPase shapes NaCl-induced systemic alkalinizations. New Phytologist **197**, 1117–1129.

**Gloser V, Korovetska H, Martín-Vertedor AI, Hájíčková M, Prokop Z, Wilkinson S, Davie W.** 2016. The dynamics of xylem sap pH under drought: a universal response in herbs? Plant and Soil **409**, 259–272.

**Gollan T, Schurr U, Schulze ED.** 1992. Stomatal response to drying soil in relation to changes in the xylem sap composition of *Helianthus annuus*. I. The concentration of cations, anions, amino acids in, and pH of the xylem sap. Plant, Cell & Environment **15**, 551–559.

**Goodger JQ, Sharp RE, Marsh EL, Schachtman DP.** 2005. Relationships between xylem sap constituents and leaf conductance of well-watered and water-stressed maize across three xylem sap sampling techniques. Journal of Experimental Botany **56**, 2389–2400.

**Hartung W.** 2010. The evolution of abscisic acid (ABA) and ABA function in lower plants, fungi and lichen. Functional Plant Biology **37**, 806–812.

**Hartung W, Radin JW, Hendrix DL.** 1988. Abscisic acid movement into the apoplastic solution of water-stressed cotton leaves: role of apoplastic pH. Plant Physiology **86**, 908–913.

**Hedrich R, Moran O, Conti F, Busch H, Becker D, Gambale F, Dreyer I, Küch A, Neuwinger K, Palme K.** 1995. Inward rectifier potassium channels in plants differ from their animal counterparts in response to voltage and channel modulators. European Biophysics Journal **24**, 107–115.

**Holbrook NM, Shashidhar VR, James RA, Munns R.** 2002. Stomatal control in tomato with ABA-deficient roots: response of grafted plants to soil drying. Journal of Experimental Botany **53**, 1503–1514.

**Jia W, Davies WJ.** 2007. Modification of leaf apoplastic pH in relation to stomatal sensitivity to root-sourced abscisic acid signals. Plant Physiology **143**, 68–77.

**Jordan JD, Landau EM, Iyengar R.** 2000. Signaling networks: the origins of cellular multitasking. Cell **103**, 193–200.

**Karuppanapandian T, Geilfus C-M, Mühling K-H, Novák O, Gloser V.** 2017. Early changes of the pH of the apoplast are different in leaves, stem and roots of *Vicia faba* L. under declining water availability. Plant Science **255**, 51–58.

**Korovetska H, Novák O, Jůza O, Gloser V.** 2014. Signalling mechanisms involved in the response of two varieties of *Humulus lupulus* L. to soil drying: I. Changes in xylem sap pH and the concentrations of abscisic acid and anions. Plant and Soil **380**, 375–387.

**Kuromori T, Sugimoto E, Shinozaki K.** 2014. Intertissue signal transfer of abscisic acid from vascular cells to guard cells. Plant Physiology **164**, 1587–1592.

**Li W, de Ollas C, Dodd IC.** 2018. Long-distance ABA transport can mediate distal tissue responses by affecting local ABA concentrations. Journal of Integrative Plant Biology **60**, 16–33.

**Manzi M, Lado J, Rodrigo MJ, Zacarías L, Arbona V, Gómez-Cadenas A.** 2015. Root ABA accumulation in long-term water-stressed plants is sustained by hormone transport from aerial organs. Plant & Cell Physiology **56**, 2457–2466.

**Marten H, Hedrich R, Roelfsema MR.** 2007. Blue light inhibits guard cell plasma membrane anion channels in a phototropin-dependent manner. The Plant Journal **50**, 29–39.

**McAdam SA, Brodribb TJ, Ross JJ.** 2016*c*. Shoot-derived abscisic acid promotes root growth. Plant, Cell & Environment **39**, 652–659.

**McAdam SA, Manzi M, Ross JJ, Brodribb TJ, Gómez-Cadenas A.** 2016*a*. Uprooting an abscisic acid paradigm: shoots are the primary source. Plant Signaling & Behavior **11**, 652–659.

**McAdam SA, Sussmilch FC, Brodribb TJ.** 2016*b*. Stomatal responses to vapour pressure deficit are regulated by high speed gene expression in angiosperms. Plant, Cell & Environment **39**, 485–491.

**Michard E, Simon AA, Tavares B, Wudick MM, Feijó JA.** 2016. Signaling with ions: the keystone for apical cell growth and morphogenesis in pollen tubes. Plant Physiology **173**, 91–111.

**Monshausen GB, Bibikova T, Messerli M, Shi C, Gilroy S.** 2007. Oscillations in extracellular pH and reactive oxygen species modulate tip growth of Arabidopsis root hairs. Proceedings of the National Academy of Sciences, USA **104**, 20996–21001.

**Monshausen GB, Bibikova TN, Weisenseel MH, Gilroy S.** 2009. $Ca^{2+}$ regulates reactive oxygen species production and pH during mechanosensing in Arabidopsis roots. The Plant Cell **21**, 2341–2356.

**Monshausen GB, Messerli MA, Gilroy S.** 2008. Imaging of the Yellow Cameleon 3.6 indicator reveals that elevations in cytosolic $Ca^{2+}$ follow oscillating increases in growth in root hairs of Arabidopsis. Plant Physiology **147**, 1690–1698.

**Munns R.** 2002. Comparative physiology of salt and water stress. Plant, Cell & Environment **25**, 239–250.

**Pfaffl MW.** 2001. A new mathematical model for relative quantification in real-time RT–PCR. Nucleic Acids Research **29**, e45.

**Plieth C.** 2016. Calcium, metaphors, and zeitgeist in plant sciences. Plant Physiology **171**, 1790–1793.

**Roelfsema MR, Hedrich R.** 2005. In the light of stomatal opening: new insights into 'the Watergate'. New Phytologist **167**, 665–691.

**Schurr U, Gollan T, Schulze ED.** 1992. Stomatal response to drying soil in relation to changes in the xylem sap composition of *Helianthus annuus*. II. Stomatal sensitivity to abscisic acid imported from the xylem sap. Plant, Cell & Environment **15**, 561–567.

**Seo M, Koshiba T.** 2002. Complex regulation of ABA biosynthesis in plants. Trends in Plant Science **7**, 41–48.

**Sharp RG, Davies WJ.** 2009. Variability among species in the apoplastic pH signalling response to drying soils. Journal of Experimental Botany **60**, 4363–4370.

**Slovik S, Hartung W.** 1992. Stress-induced redistribution kinetics of ABA in leaves: model considerations. In: Karssen CM, van Loon LC, Vreugdenhil D, eds. Progress in plant growth regulation. Current plant science and biotechnology in agriculture, vol **13**. Springer, 464–473.

**Sobeih WY, Dodd IC, Bacon MA, Grierson D, Davies WJ.** 2004. Long-distance signals regulating stomatal conductance and leaf growth in tomato (*Lycopersicon esculentum*) plants subjected to partial root-zone drying. Journal of Experimental Botany **55**, 2353–2363.

**Stoll M, Loveys B, Dry P.** 2000. Hormonal changes induced by partial rootzone drying of irrigated grapevine. Journal of Experimental Botany **51**, 1627–1634.

**Tan BC, Joseph LM, Deng WT, Liu L, Li QB, Cline K, McCarty DR.** 2003. Molecular characterization of the Arabidopsis 9-cis epoxycarotenoid dioxygenase gene family. The Plant Journal **35**, 44–56.

**Tan BC, Schwartz SH, Zeevaart JA, McCarty DR.** 1997. Genetic control of abscisic acid biosynthesis in maize. Proceedings of the National Academy of Sciences, USA **94**, 12235–12240.

**Thompson AJ, Jackson AC, Parker RA, Morpeth DR, Burbidge A, Taylor IB.** 2000. Abscisic acid biosynthesis in tomato: regulation of zeaxanthin epoxidase and 9-cis-epoxycarotenoid dioxygenase mRNAs by light/dark cycles, water stress and abscisic acid. Plant Molecular Biology **42**, 833–845.

**Wilkinson S.** 1999. pH as a stress signal. Plant Growth Regulation **29**, 87–99.

**Wilkinson S, Bacon MA, Davies WJ.** 2007. Nitrate signalling to stomata and growing leaves: interactions with soil drying, ABA, and xylem sap pH in maize. Journal of Experimental Botany **58**, 1705–1716.

**Wilkinson S, Corlett JE, Oger L, Davies WJ.** 1998. Effects of xylem pH on transpiration from wild-type and flacca tomato leaves. A vital role for abscisic acid in preventing excessive water loss even from well-watered plants. Plant Physiology **117**, 703–709.

**Wilkinson S, Davies WJ.** 1997. Xylem sap pH increase: a drought signal received at the apoplastic face of the guard cell that involves the suppression of saturable abscisic acid uptake by the epidermal symplast. Plant Physiology **113**, 559–573.

**Wilkinson S, Davies WJ.** 2008. Manipulation of the apoplastic pH of intact plants mimics stomatal and growth responses to water availability and microclimatic variation. Journal of Experimental Botany **59**, 619–631.

**Xiong L, Zhu JK.** 2003. Regulation of abscisic acid biosynthesis. Plant Physiology **133**, 29–36.